



HHS Public Access

Author manuscript

J Steroid Biochem Mol Biol. Author manuscript; available in PMC 2019 July 01.

Published in final edited form as:

J Steroid Biochem Mol Biol. 2018 July ; 181: 1–10. doi:10.1016/j.jsbmb.2018.02.008.

CYP27A1 acts on the pre-vitamin D3 photoproduct, lumisterol, producing biologically active hydroxy-metabolites

Robert C. Tuckey^a, Wei Li^b, Dejian Ma^b, Chloe Y. S. Cheng^a, Katie M. Wang^a, Tae-Kang Kim^c, Saowanee Jeayeng^{c,d}, and Andrzej T. Slominski^{c,e}

^aSchool of Molecular Sciences, The University of Western Australia, Perth, WA 6009, Australia

^bDepartment of Pharmaceutical Sciences, University of Tennessee Health Science Center, Memphis, TN 38163, USA ^cDepartment of Dermatology, University of Alabama at Birmingham, AL 35294, USA ^dDepartment of Pharmacology, Faculty of Medicine Siriraj Hospital, Mahidol University, Bangkok 10700, Thailand ^eVA Medical Center, Birmingham, AL 35294, USA

Abstract

Prolonged exposure of the skin to UV radiation causes previtamin D₃, the initial photoproduct formed by opening of the B ring of 7-dehydrocholesterol, to undergo a second photochemical reaction where the B-ring is reformed giving lumisterol₃ (L₃), a stereoisomer of 7-dehydrocholesterol. L₃ was believed to be an inactive photoproduct of excessive UV radiation whose formation prevents excessive vitamin D production. Recently, we reported that L₃ is present in serum and that CYP11A1 can act on L₃ producing monohydroxy- and dihydroxy-metabolites which inhibit skin cell proliferation similarly to 1 α ,25-dihydroxyvitamin D₃. In this study we tested the ability of human CYP27A1 to hydroxylate L₃. L₃ was metabolized by purified CYP27A1 to 3 major products identified as 25-hydroxyL₃, (25*R*)-27-hydroxyL₃ and (25*S*)-27-hydroxyL₃, by NMR. These three products were also seen when mouse liver mitochondria containing CYP27A1 were incubated with L₃. The requirement for CYP27A1 for their formation by mitochondria was confirmed by the inhibition of their synthesis by 5 β -cholestane-3 α ,7 α ,12 α -triol, an intermediate in bile acid synthesis which serves as an efficient competitive substrate for CYP27A1. CYP27A1 displayed a high k_{cat} for the metabolism of L₃ (76 mol product/min/mol CYP27A1) and a catalytic efficiency (k_{cat}/K_m) that was 260-fold higher than that for vitamin D₃. The CYP27A1-derived hydroxy-derivatives inhibited the proliferation of cultured human melanoma cells and colony formation with IC₅₀ values in the nM range. Thus, L₃ is metabolized efficiently by CYP27A1 with hydroxylation at C25 or C27 producing metabolites potent in their ability to inhibit melanoma cell proliferation, supporting that L₃ is a prohormone which can be activated by CYP-dependent hydroxylations.

Address for correspondence: Robert C. Tuckey, PhD, School of Molecular Sciences, The University of Western Australia, Perth, WA, 6009, Australia, Tel: 61 8 64883040, Fax: 61 8 30401148, robert.tuckey@uwa.edu.au.

Publisher's Disclaimer: This is a PDF file of an unedited manuscript that has been accepted for publication. As a service to our customers we are providing this early version of the manuscript. The manuscript will undergo copyediting, typesetting, and review of the resulting proof before it is published in its final citable form. Please note that during the production process errors may be discovered which could affect the content, and all legal disclaimers that apply to the journal pertain.

Conflict of Interest: The authors declare no conflict of interest

Keywords

Lumisterol; CYP27A1; hydroxylumisterol; melanoma; vitamin D; hydroxylation

1. Introduction

Vitamin D₃ is formed in the skin from the photochemical opening of the B ring of 7-dehydrocholesterol (7DHC) following the absorption of UVB (290–315 nm) radiation [1–4]. The initial photo-product of ring opening is pre-vitamin D₃ which is converted to vitamin D₃ by a first-order thermal isomerization with a half time of 2.5 h at skin temperature (37°C) [4]. Prolonged UVB radiation causes the photochemical isomerization of pre-vitamin D₃ to lumisterol₃ (L₃) and tachysterol₃ (T₃), countering excessive production of vitamin D₃ [1,5]. Further UV irradiation of T₃ favours its conversion to L₃ via pre-vitamin D₃, so that L₃ is the dominant product following extended exposure of skin to UV light [3,6]. The UV-dependent photosynthesis of L₃ from pre-vitamin D₃ involves the reformation of the C₉–C₁₀ bond to reseal the B-ring, but in a 9 β ,10 α -configuration making it a stereoisomer of 7DHC.

L₃ has long been considered to be an inactive end product of over radiation of 7DHC and does not influence calcium metabolism [5,6]. However, we have recently discovered that it can be hydroxylated on its side chain by CYP11A1 [7], a steroidogenic enzyme expressed in human skin [8–10], producing 20-hydroxyL₃, 22-hydroxyL₃, 24-hydroxyL₃ and 20,22-dihydroxyL₃ and a small amount of pregnalumisterol (pL, lumisterol with a pregnenolone-like side chain). Furthermore, we have discovered that both L₃ and its major CYP11A1-derived products are present in human serum, with the L₃ concentration being approximately 10-fold higher than that of vitamin D₃ [11]. The hydroxylumisterols are biologically active on skin cells, inhibiting proliferation and stimulating differentiation at concentrations of 10⁻⁸ to 10⁻¹¹ M, with evidence that they can act on the nongenomic site of the VDR and act as inverse agonists on ROR α and γ [11]. Chemically synthesized lumisterol derivatives, including pL and 1,25-dihydroxyL₃, have also been reported to be biologically active with the former inhibiting the proliferation and stimulating the differentiation of leukemia cells [12], and the latter protecting against skin photocarcinogenesis in a mouse model [13].

Like CYP11A1, CYP27A1 is a mitochondrial enzyme and can act on cholesterol, 7DHC and vitamin D₃ [14–17]. It catalyses 25-hydroxylation of vitamin D₃ and 27-hydroxylation of cholesterol and 7DHC. Note that C₂₆ and C₂₇ of cholesterol are equivalent carbons so CYP27A1 is sometimes referred to as sterol 26-hydroxylase rather than 27-hydroxylase. Hydroxylation at either C₂₆ or C₂₇ creates an asymmetric site at C₂₅. CYP27A1 is highly expressed in liver where its principle role is believed to be in the synthesis of bile acids where it displays high 27-hydroxylase activity on 5 β -cholestane-3 α ,7 α ,12 α -triol, producing 5 β -cholestane-3 α ,7 α ,12 α , 27-tetrol [14,18]. It can further oxidize this metabolite to the C₂₇ acid [18,19]. Its ability to convert vitamin D₃ to 25-hydroxyvitamin D₃ (25(OH)D₃) is believed to be secondary to that of CYP2R1 and deficiency results in cerebrotendinous xanthomatosis where there is altered cholesterol and bile acid metabolism, but not

25(OH)D₃ deficiency [20–22]. CYP27A1 is expressed in skin [20,23–25] which does not produce bile acids so its role is therefore thought to be in local production of 25(OH)D₃. In the current study we tested the ability of CYP27A1 to metabolize L3 and found it does this with very high catalytic efficiency, primarily producing 25-hydroxyL3 and the two epimers (25*R* and 25*S*) of 27-hydroxyL3, all of which displayed the ability to inhibit melanoma cell proliferation.

2. Materials and methods

2.1. Materials

Dioleoyl phosphatidylcholine and bovine heart cardiolipin were from Avanti Polar Lipids (Alabaster, AL). 2-Hydroxypropyl- β -cyclodextrin (HP- β -CD) was from Cerestar (Hammond, IN). Vitamin D₃, NADPH and isocitric acid (tri-sodium salt) were from Sigma-Aldrich (Sydney, Australia) and 5 β -cholestane-3 α ,7 α ,12 α -triol was from Steraloids (Newport, RI). Lumisterol₃ (L3) was purchased from Toronto Research Chemicals (Toronto, Canada) and was purified before use on a Brownlee Aquapore C18 column (25 cm \times 1 cm, 10 μ m particle size) using a gradient of methanol in water (64–100% methanol) for 15 min followed by 100% methanol for 45 min at a flow rate of 1.5 ml/min. (25*R*)-27-Hydroxycholesterol and (25*S*)-27-hydroxycholesterol were from Cayman Chemical (Ann Arbor, MI).

Human CYP27A1 with the N-terminal mitochondrial target sequence removed and a six histidine tag added to the C-terminus was expressed in *E. coli* and purified by Ni affinity- and octyl Sepharose-chromatography, as described previously [26]. Human adrenodoxin reductase, and mouse and human adrenodoxin were also expressed in *E. coli* and purified as described before [27–30].

2.2. Measurement of CYP27A1 activity

Substrates were incorporated into the bilayer of phospholipid vesicles for activity measurements. Vesicles were prepared by adding buffer (0.5 ml of 20 mM Hepes, pH7.4, 100 mM NaCl, 0.1 mM dithiothreitol and 0.1 mM EDTA) to dioleoyl phosphatidylcholine (0.89 μ mol), cardiolipin (0.38 nmol) and substrate (L3 or vitamin D₃, see Results for amounts) in 10 \times 1.3 cm glass tubes and sonicating for 10 min in a bath-type sonicator, as before [31]. To measure activity, incubations were carried out in buffer (as above) plus vesicles (510 μ M phospholipid), adrenodoxin reductase (0.4 μ M), adrenodoxin (15 μ M), CYP27A1 (0.1 or 0.2 μ M), glucose 6-phosphate (2 mM), glucose 6-phosphate dehydrogenase (2 U/ml) and NADPH (50 μ M). Samples (typically 0.5 mL) were preincubated at 37°C for 6 min and the reaction started by the addition of NADPH. At the end of the incubation at 37°C (see Results for times), reactions were terminated by the addition of 2.5 volumes of ice-cold dichloromethane. Samples were extracted 3 times with dichloromethane, as before [7], combined extracts dried under nitrogen gas and dissolved in 90% methanol in water for HPLC analysis. HPLC was carried out using a Perkin Elmer HPLC with a UV monitor and a Grace Alltima C18 column (Grace Alltima, 25 cm \times 4.6 mm, particle size 5 μ m). For L3 incubations the elution conditions were 90% methanol in water for 55 min, 90–100% methanol gradient for 2 min then 100% methanol for 55 min, at

a flow rate of 0.5 ml/min. For vitamin D3 the elution conditions were a gradient of 64–100% methanol for 15 min then 100% methanol for 50 min, at a flow rate of 0.5 ml/min. L3 and its products were monitored at 280 nm while 265 nm was used for vitamin D3. Calculations of the amounts of products formed and kinetic constants were performed as described before [32]. For some incubations the phospholipid vesicles were replaced by substrates dissolved in 0.9% HP- β -CD, as described below.

2.3. Large scale incubation of CYP27A1 with lumisterol

This was done as a scaled up version of the incubations described above except that phospholipid vesicles were replaced by 100 μ M L3 dissolved in 0.9% HP- β -CD, added from a 1.7 mM stock in 15% HP- β -CD, as before [7,32]. The final volume was 30 mL and incubations were for 30 min. Products were extracted and separated by HPLC using the HPLC conditions (methanol solvent) as described above (section 2.2). The major products (2A, 2B and 3, see Results) were collected. Because products 2A and 2B were not baseline separated, each was run again in the same solvent system and collected, to ensure high purity. Product 3 was further purified on the same column using a gradient of acetonitrile in water (45–100%) for 15 min followed by 100% acetonitrile for 45, min at a flow rate of 0.5 ml/min. The amount of each product was measured from its UV spectrum using an extinction coefficient of 8886 M⁻¹cm⁻¹ at 280 nm [33]. The collected products were further analyzed by mass spectrometry and NMR, as below.

2.4. Metabolism of lumisterol by mouse liver mitochondria

Mouse liver mitochondria were isolated as described before [34] except that the mitochondrial fraction was washed twice by resuspending it in 0.25 M sucrose and sedimenting at 6000 \times g for 15 min at 4°C. The final mitochondrial pellet was resuspended in 0.25 M sucrose to a concentration of 8 mg protein/ml and stored frozen at –8°C. For some experiments mitochondria were disrupted by sonication prior to use. An aliquot (4.5 ml) was sonicated for five 10 s bursts with 2 min cooling on ice in-between, using a Vibra Cell Ultrasonic Processor (Sonics and Materials, Inc., Newtown, CT) with a 1.2 cm probe, at 20% maximum amplitude.

Incubations of mitochondria with L3 were carried out in buffer comprising 0.25 M sucrose, 50 mM HEPES (pH 7.4), 20 mM KCl, 5 mM MgSO₄, 0.2 mM EDTA and 1.0 mg/ml fatty acid-free bovine serum albumin [24,27]. L3, dissolved in 4.5% HP- β -CD, was added from a 10-times stock giving a final HP- β -CD concentration of 0.45%. 5 β -Cholestane-3 α ,7 α ,12 α -triol, when present, was added from an ethanol stock to a final concentrations of 50 μ M or 150 μ M and a final ethanol concentration of 1.5%. Samples were preincubated for 6 min at 37°C and the reaction started by the addition of NADPH (0.5 mM) and isocitrate (5 mM). After incubation at 37°C for 60 min, reactions were terminated by the addition of 2.5 vol ice-cold dichloromethane and extracted as described above (section 2.2) for incubations with purified CYP27A1. HPLC analysis was also carried out as for incubations with purified CYP27A1.

2.5. Mass spectrometry of products

The molecular masses of the 3 major products and 1 minor product of CYP27A1 action on L3 were determined using a Waters Xevo G2-SQToF Mass Spectrometer (Waters, Milford, MA) utilizing an ESI source, and coupled with a Waters Acquity I-Class UPLC, which was equipped with a BEH C18 column (2.1 mm x 50 mm, 1.7 μ m, Waters, Milford, USA). Data were collected and processed using Masslynx 4.1 software.

2.6. NMR spectroscopy

NMR measurements were performed on 100 μ g of each of the three major products of CYP27A1 action on L3. The following 2D NMR experiments were performed: homonuclear ^1H - ^1H correlation spectroscopy (COSY), ^1H - ^1H total correlation spectroscopy (TOCSY, mixing time=80 ms), ^1H - ^1H nuclear Overhauser spectroscopy (NOESY, mixing time=300 ms), ^1H - ^{13}C heteronuclear single quantum correlation spectroscopy (HSQC), and ^1H - ^{13}C heteronuclear multiple bond correlation spectroscopy (HMBC). All NMR data were collected using a Bruker Avance III 400 MHz, with a BBO 5 mm probe with Z-gradient (Bruker BioSpin, Billerica, MA). The Bruker spectrometer was equipped with an Autosampler. IconNMR Automation within TopSpin 3.0 was used for data acquisition. Each of the three samples (100 μ g) was dissolved in 0.2 ml CD_3OD and transferred into a solvent matched 5 mm Shigemi NMR tube (Shigemi Inc., Allison Park, PA, USA). NMR data were collected at 25°C. Chemical shifts were referenced to residual solvent peaks for CD_3OD (3.31 ppm for proton and 49.15 ppm for carbon).

2.7. Cell Culture

To measure the effects of hydroxylumisterols on SKMEL-188 melanoma proliferation, 1,000 cells were grown using Ham's F10 medium containing 5% charcoal-treated FBS in 96 plates for 24 h, then synchronized for 24 h without serum. Cells were treated with hydroxylumisterols (or ethanol vehicle for control) for 72 h and analysed with MTS reagent (Promega, Madison, WI) following the manufacturer's protocol. For the colony forming assay, 500 cells were grown using Ham's F10 medium containing 5% charcoal-treated FBS in 6 well plates for 24 h then treated with the hydroxylumisterols for 6 days in the same media. The cells were fixed with ice-cold methanol for 10 min followed by adding 0.5 % crystal violet solution. Cells were incubated at room temperature for 10 min then rinsed in water until no color appeared in the rinse. Colonies were counted using Cytation 5 (BioTek Instruments, Inc., Winnoski, VT).

3. Results

3.1. Metabolism of lumisterol by CYP27A1

Initially we tested the ability of CYP27A1 to metabolize L3 incorporated into phospholipid vesicles made from dioleoyl phosphatidylcholine and cardiolipin, a system that mimics the natural environment of the enzyme in the inner mitochondrial membrane [31,32], which we have used previously to study CYP27A1 [26]. Incubation of L3 with CYP27A1 produced three major products, designated 2A, 2B and 3, plus a small complex peak with a shorter retention time comprising at least 5 unresolved products based on peak shape (Fig. 1). No

products were present in a control incubation with adrenodoxin omitted (Fig. 1A). The reverse phase HPLC conditions used to separate products 2A and 2B comprised 90% methanol in water (isocratic) on a 25 cm C18 column for 50 min, they did not separate with a 15 min methanol gradient (64–100%) initially used to analyze products, with 2A appearing as a shoulder on the 2B peak (not shown). They ran as a single peak using an acetonitrile in water gradient on the same column.

A time course for metabolism of L3 in phospholipid vesicles showed that there is rapid initial product formation, with total product formation being essentially linear for 10 min. This is followed by a marked decline in the rate for the remaining 20 min of incubation, with no further accumulation of products 2B and 3 (Fig. 1D). The complex peak of short retention time products was not observed until after 5 min of incubation, indicating that it represents secondary products formed from the further metabolism of products 2A, 2B, and/or 3. By the end of the 30 min incubation, 31% of the L3 substrate had been consumed.

In order to improve the total conversion of L3 to products to enable enzymatic synthesis of sufficient of the major products to permit structure determination by NMR, we tested the metabolism of L3 dissolved in HP- β -CD. This cyclodextrin can hold high concentrations of hydrophobic steroids or secosteroids in solution [35] and has been used by us previously for the efficient enzymatic synthesis of products for NMR using CYP27A1 [26] and other CYP enzymes [29,36]. Good conversion of L3 to products was seen with this system (Fig. 1C) with the same major products being observed as with phospholipid vesicles. In addition, a minor peak with RT= 60.7 min (product 1) was observed representing 0.8% of the total sterols (Fig. 1C). This was also just detectable in the reaction in phospholipid vesicles when the response axis was expanded (not shown). The time course for L3 metabolism with HP- β -CD (Fig. 1E) reveals that 89.7% of the substrate was consumed by the end of the 30 min incubation. The three major products decreased from 15 to 30 min of incubation as the short retention time (secondary) products increased.

The maximum yield of primary products with HP- β -CD was seen at 15 min of incubation (19.0% 2A, 41.1% 2B and 15.8% product 3). Therefore, 15 min was used under the conditions listed for Fig. 1E for scaling up the incubation to 30 mL to make sufficient products for NMR. Following HPLC purification (see Materials and Methods), 400 nmol of product 2A, 980 nmol product 2B and 290 nmol product 3 were obtained, as well as 15 nmol of the minor product 1.

3.2. Determination of the structures of major products of CYP27A1 action on L3 as 25(OH)L3 and the two epimers of 27(OH)L3

Molecular masses of the three major products were measured by high resolution MS and the results indicate that all three are mono-hydroxylumisterols (Fig. S1). They all showed ions corresponding to the mono-hydroxylumisterol complexed to Na^+ , at $m/z = 423.3252$, 423.3243, and 423.3235 for products 2A, 2B, and 3, respectively. In addition, products 2A and 2B showed ions of $[\text{M} + \text{H}]^+$ and $[\text{M} - \text{H}_2\text{O} + \text{H}]^+$, while product 3 showed abundant ions of $[\text{M} - \text{H}_2\text{O} + \text{H}]^+$ and $[\text{M} - (\text{H}_2\text{O}) + \text{H}]^+$. All the observed mass values were within 3.1 ppm compared to the calculated exact mass values, as shown in the supplemental Fig. S1.

1D proton NMR data for the three major monohydroxyL3 products are shown in Fig. 2 along with the elucidated structures. The structures were determined based on 2D NMR data as described previously [26]. For product 3, five methyl groups (positions 18, 19, 21, 26 and 27) were assigned based on HSQC and HMBC (Fig. 3). The signals for the 26 and 27 methyl groups overlapped completely. It was shown that the 26/27 carbon chemical shifts occurred at 29 ppm, a downfield shift of more than 10 ppm relative to the normal value, indicating that there is a hydroxy group near the 26 and 27 methyl groups. On HMBC, 26/27 methyl proton signals showed strong correlation with carbon peaks at 45.3 ppm, 71.4 ppm and 29.1 ppm. Based on HSQC, the peak at 71.4 ppm is confirmed as a quaternary carbon and the signal at 45.3 ppm is assigned to a methine group. The peak at 29.1 ppm is due to a methyl group. Combining these results, 71.4 ppm was assigned to carbon 25 and 45.3 ppm to carbon 24 while 29.1 ppm is due to correlation between the two methyl groups, 26 and 27. Therefore the structure of Product 3 was determined to be 25-hydroxyL3 (25(OH)L3).

Similar 2D NMR strategies were used to assign product 2A as a 27-hydroxyL3 (Fig. 3). On HMBC, 3 out of the 4 methyl groups were easily assigned to positions 18, 19, and 21. The fourth methyl group is one of the two terminal methyl groups (26 or 27). Unlike product 3, the signal is not the overlap of both 26 and 27 methyls because there is no HMBC correlation from the methyl proton to a methyl carbon. Instead, it shows strong correlation to carbon peaks at 34.7, 36.8, and 68.4 ppm. HSQC showed that the 36.8 ppm carbon is a methine group, while both carbons at 34.7 and 68.4 ppm are methylene groups. For positions 24, 25 and one of the terminal methyl carbons, the only possibility for the 68.4 ppm would be a terminal methyl carbon (C27) with one proton replaced with an hydroxy group. Signals at 34.7 and 36.8 ppm were subsequently assigned to positions 24 and 25, respectively. Product 2B gave very similar NMR data to product 2A (Fig. 2, HSQC and Fig. S12, HMBC) and was determined as the second stereoisomer of 27-hydroxyL3. Supporting NMR data for identifications are shown in Figs S3–S27.

NOESY NMR spectra were acquired to distinguish the stereochemistry at C25 of products 2A and 2B. Both were initially defined as 27-hydroxyL3, as described above. The NOE cross-peak between 24H₂ and 26CH₃ showed weaker intensity in 2A than 2B (Fig. 4). 24H₂ is a little further away from the side chain 26CH₃ group in the 25*S* structure than in the 25*R* structure, as shown in the model (Fig. S2). Therefore, product 2A is (25*S*)-27-hydroxyL3 ((25*S*)-27(OH)L3), and 2B is (25*R*)-27-hydroxyL3 ((25*R*)-27(OH)L3).

To further confirm the above results, NMR data were acquired on (25*R*)-27-hydroxycholesterol and (25*S*)-27-hydroxycholesterol for comparison to the corresponding lumisterol products. The two hydroxycholesterol stereoisomers showed very similar HSQC spectra to each other with differences only at C23 and C24. Comparing the chemical shifts from this pair of standards with those of products 2A and 2B (Table 1) further confirms that product 2A is the (25*S*)- and 2B is the (25*R*)-isomer of 27(OH)L3. Chemical shifts of all carbons and protons were assigned, except the quaternary carbon C8 for all three major products (Table S1). Molecular masses of all three major products, measured by high resolution MS, were consistent with the NMR data (Fig. S1).

Lastly, the HRMS of the additional minor product (product 1, Fig. 2) gave the parent ion ($[M + Na]^+$) = 421.3076, two mass units less than the major products which suggests that it is an aldehyde formed from one of the stereoisomers of 27(OH)L3 (Fig. S1). This is consistent with the known ability of CYP27A1 to carry out this type of oxidation, for example the conversion of 27-hydroxycholesterol to 3 β -hydroxy-5-cholesten-27-al [37]. An insufficient amount of product 1 was available to carry out NMR to confirm its structure.

3.3. Kinetics of lumisterol metabolism in phospholipid vesicles

To determine the kinetic constants for L3 metabolism by CYP27A1, substrate was dissolved in the membrane of phospholipid vesicles. Because the substrate is in the phospholipid bilayer and not in the aqueous phase, K_m values are expressed as molar ratios of substrate to phospholipid [26,30,31,36,38]. The initial rates of metabolism of L3 by human CYP27A1 showed a good fit to the Michaelis-Menten equation giving $K_m = 0.37 \pm 0.08$ mol L3/mol phospholipid (data are \pm SE from the curve fit) and $k_{cat} = 75.8 \pm 9.7$ mol product/mol CYP27A1/min (Fig. 5). Under identical conditions, vitamin D3, a well characterized substrate of CYP27A1 which is metabolized to 25(OH)D3 [15,20], gave $K_m = 0.59 \pm 0.18$ mol/mol phospholipid and $k_{cat} = 0.53 \pm 0.10$ mol product/mol CYP27A1/min. Therefore CYP27A1 displays a catalytic efficiency for L3 ($202 \text{ min}^{-1}(\text{mol/mol phospholipid})^{-1}$) 260-fold higher than that for vitamin D3 ($0.90 \text{ min}^{-1}(\text{mol/mol phospholipid})^{-1}$), due largely to the very much higher k_{cat} for L3 compared to vitamin D3. Thus lumisterol is an extremely good substrate for CYP27A1 compared to vitamin D3 (see Discussion).

3.4. Metabolism of L3 by mouse liver mitochondria

To further characterize the ability of CYP27A1 to metabolise L3, experiments on L3 metabolism by mouse liver mitochondria, which contain a relatively high concentration of this enzyme, were carried out. We observed that the mitochondria produced the same three products, 25(OH)L3, (25*R*)-27(OH)L3 and (25*S*)-27(OH)L3, as purified human CYP27A1 (identical retention times confirmed by spiking, not shown) and in similar proportions, approximately 1: 2.2:1.4, respectively (Fig. 6, Table 2). A small amount of short retention-time products were also seen that were not present in the control incubation (Fig. 4). Disrupting the mitochondria by sonication completely prevented product formation (Table 2). This loss of activity is most likely due to dilution of adrenodoxin and adrenodoxin reductase into the surrounding buffer, as has been observed for other mitochondrial P450s [39]. Supplementing the disrupted mitochondria with saturating concentrations of exogenous adrenodoxin and adrenodoxin reductase not only restored activity, but stimulated it by 2.7-fold compared to intact mitochondria. This enhancement of activity could be due to adrenodoxin and/or adrenodoxin reductase being limiting for CYP27A1 activity in intact liver mitochondria, as seen for CYP11A1 in the human placenta [28,39], or due to better access of the CYP27A1 to the L3 substrate when the mitochondria are disrupted. Either way, the stimulation by adrenodoxin reductase and adrenodoxin clearly demonstrates that the reaction is due to a mitochondrial P450.

To further confirm that the reaction is due to CYP27A1, incubations were done in the presence of a competitive substrate, 5 β -cholestane-3 α ,7 α ,12 α -triol, which is metabolised by CYP27A1 with high catalytic efficiency [15,19]. Because the 27-tetrol product formed from

5 β -cholestane-3 α ,7 α ,12 α -triol has no UVB absorbance it does not interfere with the HPLC assay of L3 metabolites. The 5 β -cholestane-3 α ,7 α ,12 α -triol caused a concentration-dependent inhibition of L3 metabolism in both intact and sonicated mitochondria, clearly demonstrating that L3 metabolism is due to CYP27A1. With equal concentrations of L3 and 5 β -cholestane-3 α ,7 α ,12 α -triol, L3 metabolism by disrupted mitochondria supplemented with adrenodoxin and adrenodoxin reductase was decreased by 3.1 fold, suggesting that the triol binds slightly tighter to the active site of the CYP27A1 than L3 (a 2-fold reduction would be predicted for equal binding strength).

3.5. Biological activities of 25(OH)L3 and the two epimers of 27(OH)L3

Since the CYP11A1-derived hydroxylumisterols are active on melanoma cells [10], we chose these cells for initial testing of the activities of the CYP27A1-derived hydroxylumisterols. All three, 25(OH)L3, (25*R*)-27(OH)L3 and (25*S*)-27(OH)L3 inhibited SKMEL-188 melanoma cell proliferation with high potency ($IC_{50} = 10^{-9}$ to 10^{-10} M), as determined with MTS reagent which measures mitochondrial activity (Fig. 7A). They also inhibited colony formation by these cells with similar potencies (Fig. 7B).

4. Discussion

This study reveals that CYP27A1 efficiently metabolizes L3 to 25(OH)L3, (25*R*)-27(OH)L3 and (25*S*)-27(OH)L3. The k_{cat} we observed (76 min^{-1}) for metabolism of lumisterol by CYP27A1 is similar to or higher than that of the best known substrate for CYP27A1, the bile acid intermediate 5 β -cholestane-3 α ,7 α ,12 α -triol. This bile acid intermediate has been reported to be hydroxylated at C27 with a k_{cat} of 23 min^{-1} for the enzyme purified from rabbit liver mitochondria [19] and 39 min^{-1} for one study with the recombinant human enzyme [14] and $70\text{--}80 \text{ min}^{-1}$ in another [40]. It is not possible to directly compare the catalytic efficiency (k_{cat}/K_m) of CYP27A1 for metabolism of L3 and 5 β -cholestane-3 α ,7 α ,12 α -triol because of the different assay systems employed. However, our data on inhibition of L3 metabolism by 5 β -cholestane-3 α ,7 α ,12 α -triol using disrupted liver mitochondria suggest that 5 β -cholestane-3 α ,7 α ,12 α -triol binds to CYP27A1 only slightly stronger than L3, suggesting the enzyme has comparable k_{cat}/K_m values for these two substrates.

In the current study we show that L3 is metabolized by CYP27A1 with a catalytic efficiency 260-fold higher than the well characterized 25-hydroxylation of vitamin D3, primarily due to a much higher k_{cat} value, with K_m values for vitamin D3 and L3 being comparable. L3 is also metabolized with a catalytic efficiency 10-fold higher than for 27-hydroxylation of cholesterol, the latter being determined previously under identical conditions to the current study [26].

We have recently reported that L3 is present in human serum at a concentration 10 times higher than that of vitamin D3 [11]. Thus serum-derived L3 should be available to the liver for conversion to hydroxylumisterols. However, the rate of L3 metabolism by liver CYP27A1 may be limited by competition with locally produced 5 β -cholestane-3 α ,7 α ,12 α -triol, and to a lesser extent cholesterol, due to the high concentrations of these sterols in the liver mitochondria. In contrast, in the skin L3 is likely to be a major substrate for CYP27A1, particularly after extended exposure to UVB radiation, with the lumisterol being

metabolized much more efficiently than either cholesterol, vitamin D3 or 7DHC [17,26]. The L3 concentration in human skin is 13-fold higher than the D3 concentration but lower than the 7DHC concentration [11]. Relative local concentrations of these sterols in the mitochondria of the different cell types present in the epidermis are unknown.

We have previously reported that L3 is hydroxylated at C20, C22 and C24 by purified bovine and human CYP11A1, and by adrenal fragments containing CYP11A1 [7]. Comparison of the rate of L3 metabolism between that study and the current one reveals that the k_{cat} for L3 metabolism by human CYP27A1 is 16 times higher than the k_{cat} of bovine CYP11A1 for metabolism of L3, and even higher versus human CYP11A1. K_m values cannot be compared due to the different assay systems used in these two studies.

From the current study L3 can be added to the list of substrates that can be acted on by CYP27A1. Besides vitamin D3, cholesterol and bile acid intermediates such as 5 β -cholestane-3 α ,7 α ,12 α -triol and 5 β -cholestane-3 α ,7 α ,12 α , 27-tetrol, human CYP27A1 in transfected COS-1 cells has been shown to act on vitamin D2 (24- and 27-hydroxylation), 1(OH)D2 (24- and 27-hydroxylation), 1(OH)D3 (mainly 25-hydroxylation), dihydrotachysterol3 and 1(OH)dihydrotachysterol3 (mainly 25-hydroxylation) [16]. Recombinant human CYP27A1 can hydroxylate 7DHC (which is a stereoisomer of lumisterol) at C25 and C27, but 5-times less conversion was seen than with cholesterol as substrate [17]. Slow metabolism of zymosterol, desmosterol and lanosterol to C27 alcohols and acids was also observed. Recently, CYP27A1 was shown to hydroxylate the side chain of β -sitosterol at C26 and C29, and ergosterol at C24, C26 and C28 [41].

In this study we have clearly shown by HPLC and NMR that both C25 stereoisomers of 27(OH)L3 are produced by CYP27A1, with the *R* isomer being favoured by a factor of approximately 2 over the *S* isomer. The absolute configurations of each of the two enantiomers was confirmed by comparison of their NMR spectra to authentic (25*R*)- and (25*S*)-27-hydroxycholesterol, available commercially. Interestingly, to our knowledge no one appears to have analysed whether 27-hydroxylation of cholesterol or 7DHC by CYP27A1 gives both C25 stereoisomers, likely due to the difficulty of separating them by chromatography. For example, in the analysis of 27-hydroxylation of 7DHC by CYP27A1, the standard used for identification was a mixture of C25 *R* and *S* isomers of 27-hydroxy-DHC and gave a single peak by reverse phase HPLC with an acetonitrile solvent system, precluding the identification of the individual isomers [42]. It has been reported that partially purified CYP27A1 from rat liver mitochondria hydroxylates 5 β -cholestane-3 α ,7 α ,12 α -triol at C27 producing 5 β -cholestane-3 α ,7 α ,12 α ,27-tetrol, exclusively with 25*R* chirality [43]. However, this stereospecificity for producing only the *R*-epimer may not apply to the hydroxylation of cholesterol or 7DHC at C27, since it does not hold for L3.

The three major products of metabolism of L3 by CYP27A1, 25(OH)L3, (25*R*)-27(OH)L3 and (25*S*)-27(OH)L3, all displayed biological activity, with initial studies showing that they inhibit melanoma cell proliferation and colony formation with IC_{50} values in the 0.2 to 5 nM concentration range. These IC_{50} values for the inhibition of proliferation are slightly higher than those for the three major monohydroxy products of L3 metabolism by CYP11A1, (IC_{50} values approximately 10^{-11} M) [11]. IC_{50} values for colony growth in soft agar for the

CYP27A1-derived hydroxylumisterols were similar to those reported for the two major products of L3 metabolism by CYP11A1, 22(OH)L3 and 24(OH)L3. Thus, the major products of CYP27A1 action on lumisterol are active on melanoma cells, and possibly other cell types to be investigated in the future. While the receptor that mediates this action remains to be identified, our recent studies on the CYP11A1-derived hydroxylumisterols suggest lumisterols hydroxylated on the side chain act through through the non-genomic site (A-pocket) of the vitamin D receptor [11], and/or through binding to ROR α and ROR γ [11,44].

In conclusion, this study shows that L3 is metabolised with high catalytic efficiency by CYP27A1 and provides further evidence that it is not an inactive end product of over-irradiation of the skin by UVB, but is a pro-hormone that can be efficiently activated by hydroxylation by CYP27A1.

Supplementary Material

Refer to Web version on PubMed Central for supplementary material.

Acknowledgments

We would like to acknowledge The University of Western Australia and the Research Training Program for their financial support to CYSC. The work was supported in part by grants from the National Institutes of Health (R21AR066505-01A1, 1R01AR071189-01A1 and 1R01AR056666-01A2) to ATS. Additional supports by grants from the National Institutes of Health (1S10OD010678-01 for the HRMS instrument, RR-026377-01 for the NMR instrument, and 1R21AR063242-01A1) to WL are also acknowledged. Partial support of the Royal Golden Jubilee Ph.D Scholarship Program (Grant number PHD/0181/2554) to SJ is also acknowledged.

Abbreviations

CYP	cytochrome P450
7DHC	7-dehydrocholesterol
20	22(OH) ₂ L3, 20,22-dihydroxylumisterol3
HP-β-CD	2-hydroxypropyl- β -cyclodextrin
25(OH)D3	25-hydroxyvitamin D3
22(OH)L3	22-hydroxylumisterol3
24(OH)L3	24-hydroxylumisterol3
25(OH)L3	25-hydroxylumisterol3
(25R)-27(OH)L3	(25R)-27-hydroxylumisterol3
(25S)-27(OH)L3	(25S)-27-hydroxylumisterol3
L3	Lumisterol3

References

1. Holick MF. Vitamin D: a millennium perspective. *J Cell Biochem.* 2003; 88:296–307. [PubMed: 12520530]
2. Holick MF, MacLaughlin JA, Clark MB, Holick SA, Potts JT Jr, Anderson RR, Blank IH, Parrish JA, Elias P. Photosynthesis of previtamin D₃ in human skin and the physiologic consequences. *Science.* 1980; 210:203–205. [PubMed: 6251551]
3. MacLaughlin JA, Anderson RR, Holick MF. Spectral character of sunlight modulates photosynthesis of previtamin D₃ and its photoisomers in human skin. *Science.* 1982; 216:1001–1003. [PubMed: 6281884]
4. Tian XQ, Chen TC, Matsouka LY, Wortsman J, Holick MF. Kinetic and Thermodynamic studies of the conversion of previtamin D₃ to vitamin D₃ in human skin. *J Biol Chem.* 1993; 268:1488–1492. [PubMed: 8419348]
5. Wacker M, Holick MF. Sunlight and vitamin D. A global perspective for health. *Dermatoendocrinol.* 2013; 5:1–58. [PubMed: 24494037]
6. Holick MF, MacLaughlin JA, Doppelt SH. Regulation of cutaneous previtamin D₃ photosynthesis in man: Skin pigment is not an essential regulator. *Science.* 1981; 211:590–593. [PubMed: 6256855]
7. Tuckey RC, Slominski AT, Cheng CYS, Chen J, Kim TK, Xiao M, Li W. Lumisterol is metabolized by CYP11A1: discovery of a new pathway. *Int J Biochem Cell Biol.* 2014; 55:24–34. [PubMed: 25130438]
8. Slominski A, Ermak G, Mihm M. ACTH receptor, CYP11A1, CYP17 and CYP21A2 genes are expressed in skin. *J Clin Endocrinol Metab.* 1996; 81:2746–2749. [PubMed: 8675607]
9. Thiboutot D, Jabara S, McAllister JM, Sivarajah A, Gilliland K, Cong Z, Clawson G. Human skin is a steroidogenic tissue: steroidogenic enzymes and cofactors are expressed in epidermis, normal sebocytes, and an immortalized sebocyte cell line (SEB-1). *J Invest Dermatol.* 2003; 120:905–914. [PubMed: 12787114]
10. Slominski A, Zjawiony J, Wortsman J, Semak I, Stewart J, Pisarchik A, Sweatman T, Marcos J, Dunbar C, Tuckey RC. A novel pathway for sequential transformation of 7-dehydrocholesterol and expression of the P450_{scc} system in mammalian skin. *Eur J Biochem.* 2004; 271:4178–4188. [PubMed: 15511223]
11. Slominski AT, Kim TK, Hobrath JV, Janjetovic Z, Oak ASW, Postlethwaite A, Lin Z, Li W, Soon H, Jetten AM, Tuckey RC. Characterization of a new pathway which activates lumisterol *in vivo* to biologically active hydroxylumisterols. *Sci Rep.* 2017; 7:11434. [PubMed: 28900196]
12. Slominski AT, Janjetovic Z, Fuller BE, Zmijewski MA, Tuckey RC, Nguyen MN, Sweatman T, Li W, Zjawiony J, Miller D, Chen TC, Lozanski G, Holick MF. Products of vitamin D₃ or 7-dehydrocholesterol metabolism by cytochrome P450_{scc} show anti-leukemia effects, having low or absent calcemic activity. *PLoS One.* 2010; 5:e9907. [PubMed: 20360850]
13. Dixon KM, Deo SS, Wong G, Slater M, Norman AW, Bishop JE, Posner GH, Ishizuka S, Halliday GM, Reeve VE, Mason RS. Skin cancer prevention: a possible role of 1,25dihydroxyvitamin D₃ and its analogs. *J Steroid Biochem Mol Biol.* 2005; 97:137–143. [PubMed: 16039116]
14. Andersson S, Davis DL, Dahlback H, Jornvall H, Russell DW. Cloning, structure, and expression of the mitochondrial cytochrome P-450 sterol 26-hydroxylase, a bile acid biosynthetic enzyme. *J Biol Chem.* 1989; 264:8222–8229. [PubMed: 2722778]
15. Pikuleva IA, Bjorkhem I, Waterman MR. Expression, purification, and enzymatic properties of recombinant human cytochrome P450_{c27} (CYP27). *Arch Biochem Biophys.* 1997; 343:123–130. [PubMed: 9210654]
16. Guo YD, Strugnell S, Black DW, Jones G. Transfected human liver cytochrome P-450 hydroxylates vitamin D analogs at different side-chain positions. *Proc Natl Acad Sci U S A.* 1993; 90:8668–8672. [PubMed: 7690968]
17. Pikuleva I, Javitt NB. Novel sterols synthesized via the CYP27A1 metabolic pathway. *Arch Biochem Biophys.* 2003; 420:35–39. [PubMed: 14622972]
18. Betsholtz IH, Wikvall K. Cytochrome P450 CYP27-catalyzed oxidation of C27-steroid into C27-acid. *J Steroid Biochem Mol Biol.* 1995; 55:115–119. [PubMed: 7577714]

19. Furster C, Bergman T, Wikvall K. Biochemical characterization of a truncated form of CYP27A purified from rabbit liver mitochondria. *Biochem Biophys Res Commun*. 1999; 263:663–666. [PubMed: 10512735]
20. Skrede S, Bjorkhem I, Kvittingen EA, Buchmann HS, Lie SO, Grundy S. Demonstration of 26-hydroxylation of C27-steroids in human skin fibroblasts, and a deficiency of this activity in cerebrotendinous xanthomatosis. *J Clin Invest*. 1986; 78:729–735. [PubMed: 3745434]
21. Zhu J, DeLuca HF. Vitamin D 25-hydroxylase – Four decades of searching, are we there yet? *Arch Biochem Biophys*. 2012; 523:30–36. [PubMed: 22310641]
22. Cheng, CYS., Kim, TK., Jeayeng, S., Slominski, AT., Tuckey, RC. Properties of purified CYP2R1 in a reconstituted membrane environment and its 25-hydroxylation of 20-hydroxyvitamin D3. *J Steroid Biochem Mol Biol*. 2017. <https://doi.org/10.1016/j.jsbmb.2017.07.011>
23. Vantieghem K, Overbergh L, Carmeliet G, De Haes P, Bouillon R, Segaert S. UVB-induced 1,25(OH)₂D₃ production and vitamin D activity in intestinal CaCo-2 cells and in THP-1 macrophages pretreated with a sterol ⁷-reductase inhibitor. *J Cell Biochem*. 2006; 99:229–240. [PubMed: 16598763]
24. Slominski AT, Kim TK, Shehabi HZ, Semak I, Tang EK, Nguyen MN, Benson HA, Korik E, Janjetovic Z, Chen J, Yates CR, Postlethwaite A, Li W, Tuckey RC. In vivo evidence for a novel pathway of vitamin D(3) metabolism initiated by P450_{scc} and modified by CYP27B1. *FASEB J*. 2012; 26:3901–3915. [PubMed: 22683847]
25. Wasiewicz T, Szyszka P, Cichorek M, Janjetovic Z, Tuckey RC, Slominski AT, Zmijewski MA. Antitumor effects of vitamin D analogs on hamster and mouse melanoma cell lines in relation to melanin pigmentation. *Int J Mol Sci*. 2015; 16:6645–6667. [PubMed: 25811927]
26. Tieu EW, Li W, Chen J, Baldisseri DM, Slominski AT, Tuckey RC. Metabolism of cholesterol, vitamin D₃ and 20-hydroxyvitamin D₃ incorporated into phospholipid vesicles by human CYP27A1. *J Steroid Biochem Mol Biol*. 2012; 129:163–171. [PubMed: 22210453]
27. Woods ST, Sadleir J, Downs T, Triantopoulos T, Headlam MJ, Tuckey RC. Expression of catalytically active human cytochrome P450_{scc} in *Escherichia coli* and mutagenesis of isoleucine-462. *Arch Biochem Biophys*. 1998; 353:109–115. [PubMed: 9578606]
28. Tuckey RC, Sadleir J. The concentration of adrenodoxin reductase limits cytochrome P450_{scc} activity in the human placenta. *Eur J Biochem*. 1999; 263:319–325. [PubMed: 10406938]
29. Tuckey RC, Li W, Shehabi HZ, Janjetovic Z, Nguyen MN, Kim TK, Chen J, Howell DE, Benson HA, Sweatman T, Baldisseri DM, Slominski A. Production of 22-hydroxymetabolites of vitamin D₃ by cytochrome P450_{scc} (CYP11A1) and analysis of their biological activities on skin cells. *Drug Metab Dispos*. 2011; 39:1577–1588. [PubMed: 21677063]
30. Tang EKY, Voo KJQ, Nguyen MN, Tuckey RC. Metabolism of substrates incorporated into phospholipid vesicles by mouse 25-hydroxyvitamin D₃ 1 α -hydroxylase (CYP27B1). *J Steroid Biochem Mol Biol*. 2010; 119:171–179. [PubMed: 20193763]
31. Tuckey RC, Kamin H. Kinetics of the incorporation of adrenal cytochrome P-450_{scc} into phosphatidylcholine vesicles. *J Biol Chem*. 1982; 257:2887–2893. [PubMed: 7061453]
32. Tuckey RC, Nguyen MN, Slominski A. Kinetics of vitamin D₃ metabolism by cytochrome P450_{scc} (CYP11A1) in phospholipid vesicles and cyclodextrin. *Int J Biochem Cell Biol*. 2008; 40:2619–2626. [PubMed: 18573681]
33. Norval M, Bjorn LO, de Grujil FR. Is the action spectrum for the UV-induced production of previtamin D₃ in human skin correct? *Photochem Photobiol*. 2010; 9:11–17.
34. Cheng CYS, Slominski AT, Tuckey RC. Metabolism of 20-hydroxyvitamin D₃ by mouse liver microsomes. *J Steroid Biochem Mol Biol*. 2014; 144:286–293. [PubMed: 25138634]
35. De Caprio J, Yun J, Javitt NB. Bile acid and sterol solubilization in 2-hydroxypropyl- β -cyclodextrin. *J Lipid Res*. 1992; 33:441–443. [PubMed: 1569391]
36. Tieu EW, Tang EK, Chen J, Li W, Nguyen MN, Janjetovic Z, Slominski A, Tuckey RC. Rat CYP24A1 acts on 20-hydroxyvitamin D(3) producing hydroxylated products with increased biological activity. *Biochem Pharmacol*. 2012; 84:1696–1704. [PubMed: 23041230]
37. Pikuleva IA, Babiker A, Waterman MR, Bjorkhem I. Activities of recombinant human cytochrome P450_{c27} (CYP27) which produce intermediates of alternative bile acid biosynthetic pathways. *J Biol Chem*. 1998; 273:18153–18160. [PubMed: 9660774]

38. Tuckey RC, Stevenson PM. Properties of bovine luteal cytochrome P-450_{sc} incorporated into artificial phospholipid vesicles. *Int J Biochem.* 1984; 16:497–503. [PubMed: 6724104]
39. Tuckey RC, Woods ST, Tajbakhsh M. Electron transfer to cytochrome P-450_{sc} limits cholesterol side-chain-cleavage activity in the human placenta. *Eur J Biochem.* 1997; 244:835–839. [PubMed: 9108254]
40. Murtazina DA, Andersson U, Hahn IS, Bjorkhem I, Ansari GA, Pikuleva IA. Phospholipids modify substrate binding and enzyme activity of human cytochrome P450 27A1. *J Lipid Res.* 2004; 45:2345–2353. [PubMed: 15342675]
41. Ehrhardt M, Gerber A, Zapp J, Hannemann F, Bernhardt R. Human CYP27A1 catalyses hydroxylation of beta-sitosterol and ergosterol. *Biol Chem.* 2016; 397:513–518. [PubMed: 26891232]
42. Endo-Umeda K, Yasuda K, Sugita K, Honda A, Ohta M, Ishikawa M, Hashimoto Y, Sakaki T, Makishima M. 7-Dehydrocholesterol metabolites produced by sterol 27-hydroxylase (CYP27A1) modulate liver X receptor activity. *J Steroid Biochem Mol Biol.* 2014; 140:7–16. [PubMed: 24269243]
43. Atsuta Y, Okuda K. On the stereospecificity of cholestanetriol monooxygenase. *J Biol Chem.* 1981; 256:9144–9146. [PubMed: 7263704]
44. Jetten AM, Takeda Y, Slominski A, Kang HS. Retinoic acid-related Orphan Receptor γ (ROR γ): connecting sterol metabolism to regulation of the immune system and autoimmune disease. *Current Opinion in Toxicology.* 2018; doi: 10.1016/j.cotox.2018.01.005

Highlights

- Purified CYP27A1 can hydroxylate the side chain of lumisterol at C25 and C27
- Both (25*R*)- and (25*S*)-27-hydroxylumisterol are products of CYP27A1
- CYP27A1 hydroxylates lumisterol with greater catalytic efficiency than vitamin D3
- CYP27A1 in liver mitochondria shows similar action on lumisterol to purified CYP27A1 CYP27A1-derived hydroxylumisterols inhibit melanoma cell proliferation

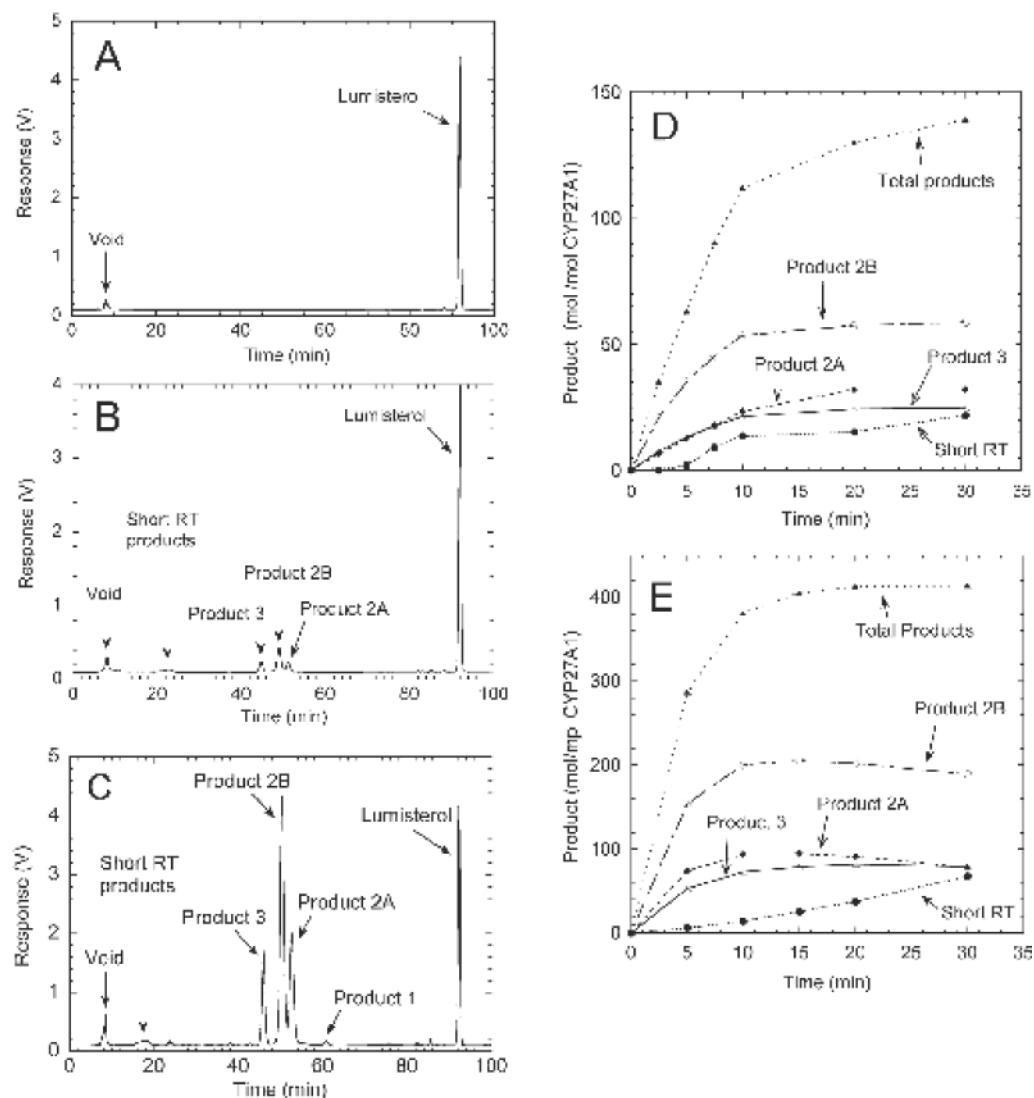


Fig. 1. CYP27A1 acts on L3 in phospholipid vesicles or HP-β-CD to produce three major products. Phospholipid vesicles containing 0.1 mol L3/mol phospholipid or L3 (100 μM) dissolved in HP-β-CD (final concentration 0.9%) were incubated with 0.2 μM CYP27A1, 0.4 μM adrenodoxin reductase, 15 μM adrenodoxin and 50 μM NADPH at 37°C. Extracted sterols were analysed by reverse phase HPLC (see Methods). (A), Control incubation of L3 in vesicles for 30 min with adrenodoxin omitted; (B) test incubation for 30 min with L3 in vesicles; (C), test incubation for 30 min with L3 in HP-β-CD; (D) time course for metabolism of L3 in phospholipid vesicles; (E) time course for the metabolism of L3 in HP-β-CD.

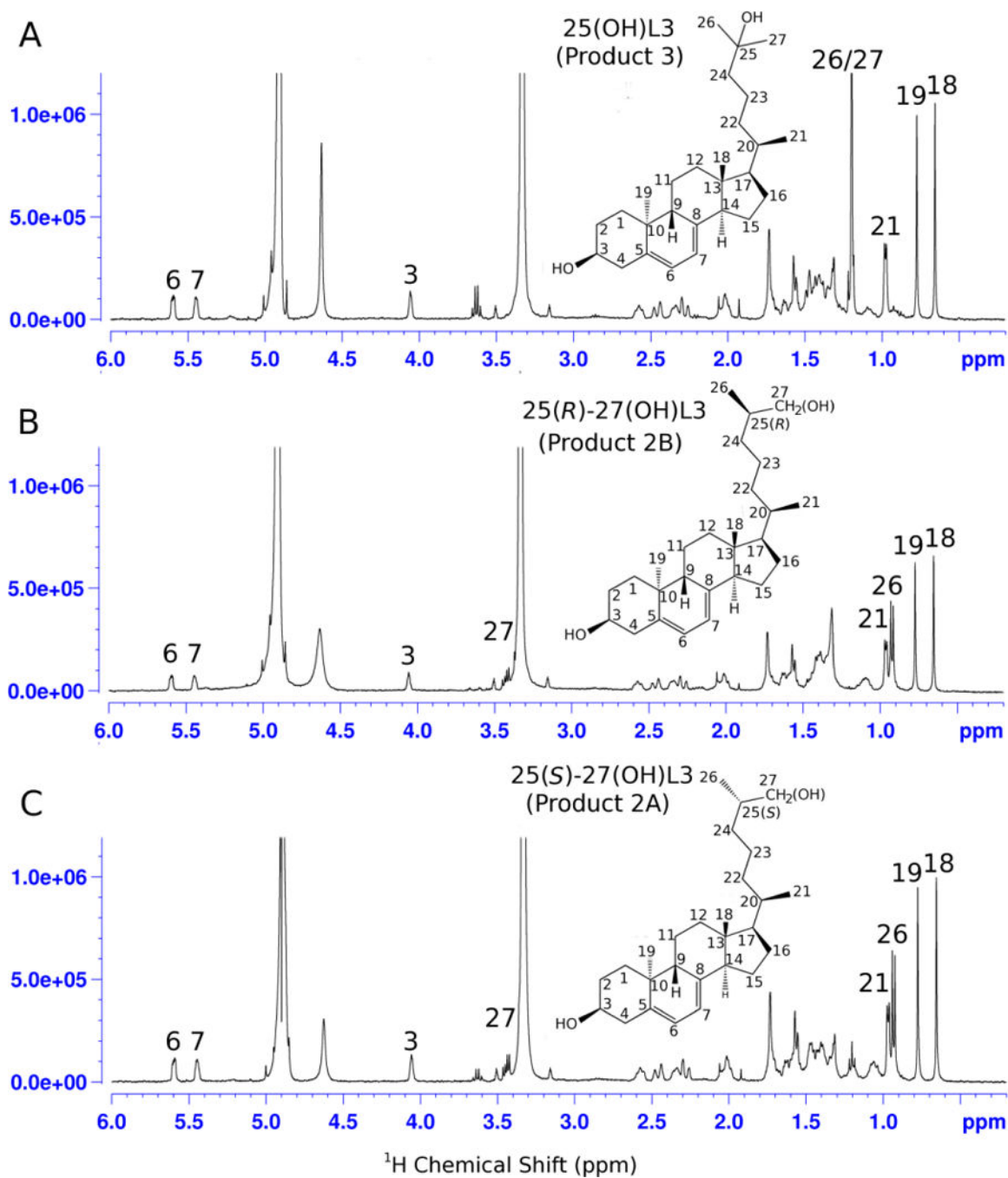


Fig. 2. ¹H NMR spectra of the three major hydroxylumisterol products. (A), Product 3 = 25-hydroxyL3; (B), product 2B = 25(*R*)-27-hydroxyL3; (C), product 2A = 25(*S*)-27-hydroxyL3. See text for a description of the identification.

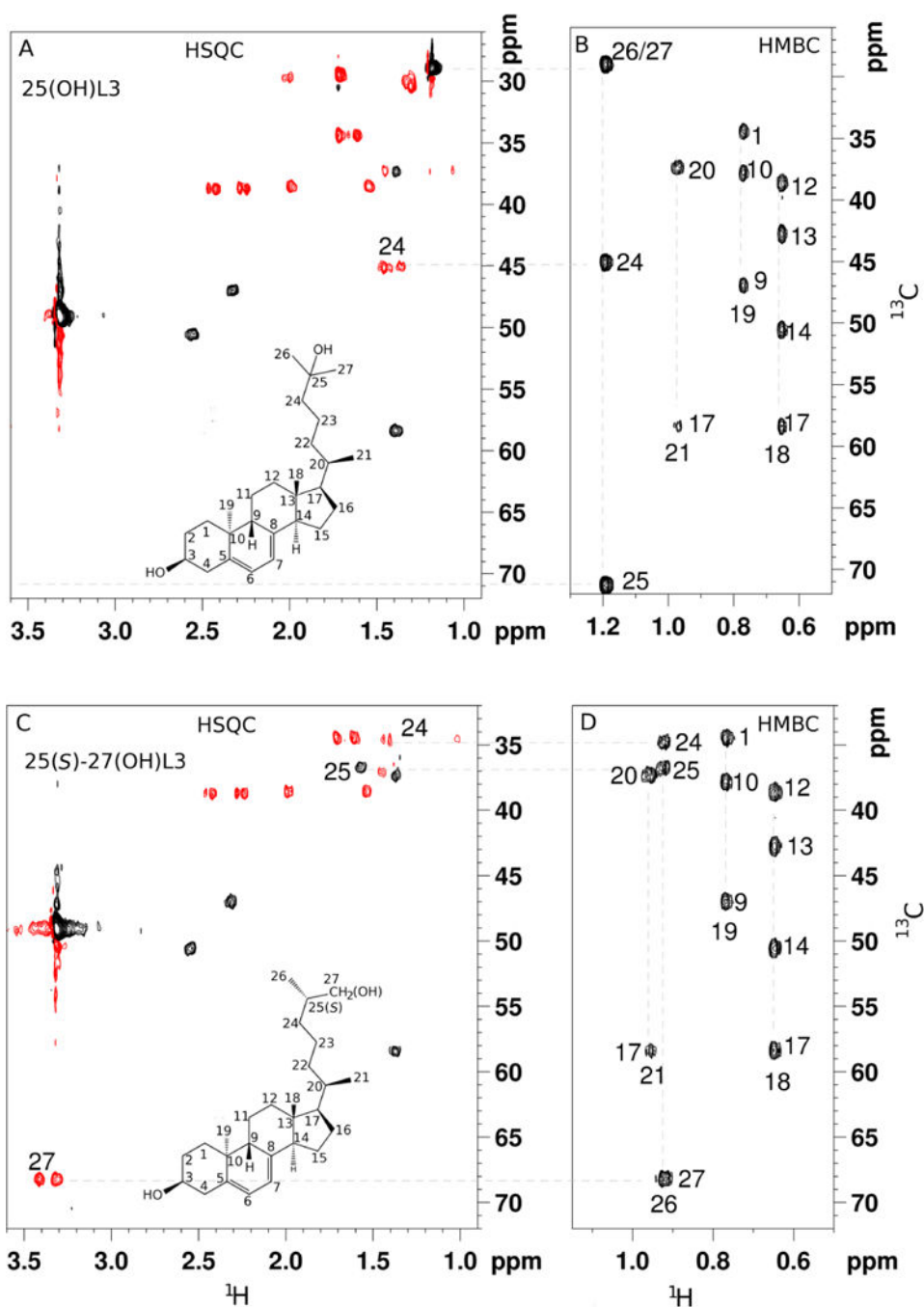


Fig. 3. HSQC and HMBC NMR spectra of the major hydroxylumisterol products. (A and B), Product 3, 25-hydroxy L3. (C and D), product 2A, 25(*S*)-27-hydroxyL3 with some key assignments. Note that no signal was observed on HSQC for C25 in 25-hydroxyL3 because it is a quaternary carbon.

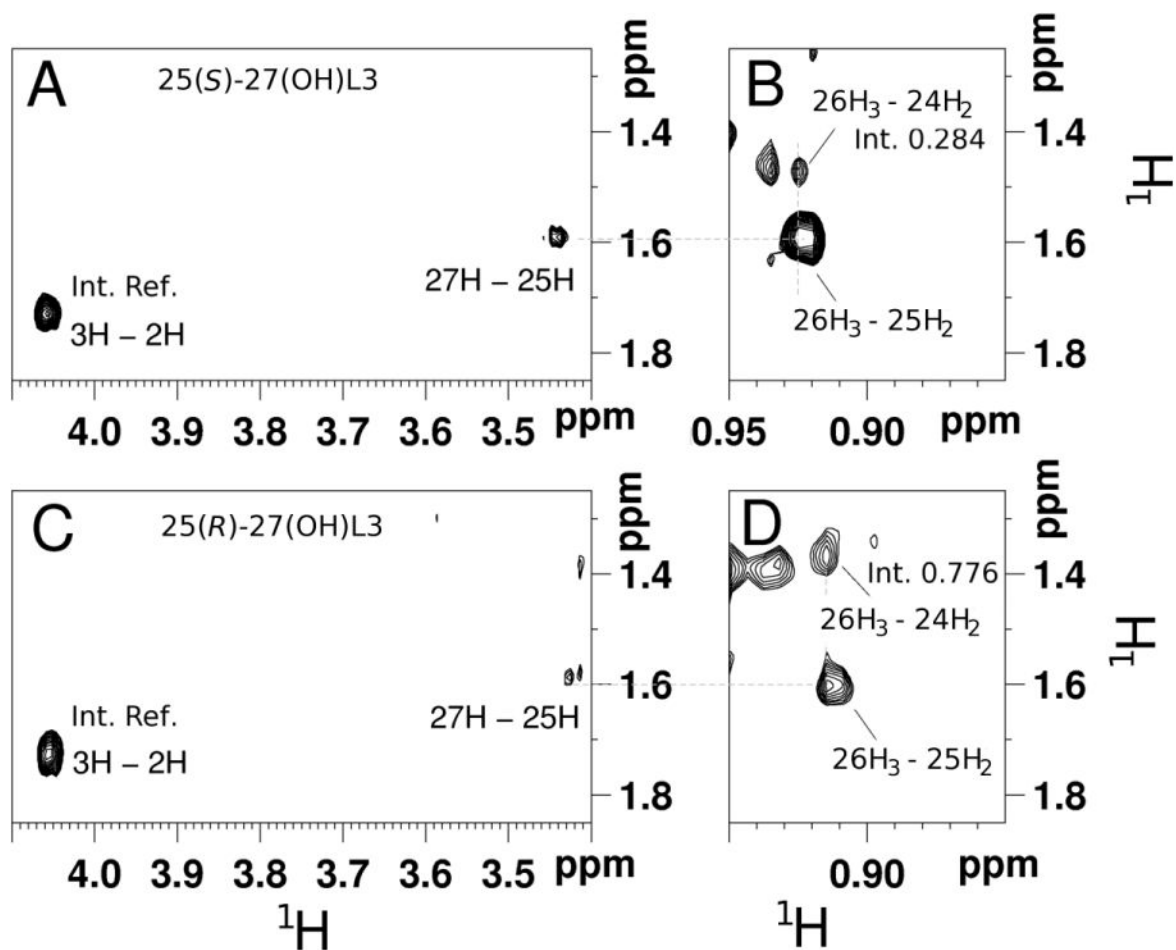


Fig. 4. NOESY NMR spectra of hydroxylumisterols. (A and B), 25(*S*)-27-hydroxyL3; (C and D), 25(*R*)-27-hydroxyL3. The relative integrals of the signals between 26H₃ and 24H₂ help to determine the stereochemistry for carbon 25. The integrals were referenced to a well-defined signal between 2H and 3H as shown.

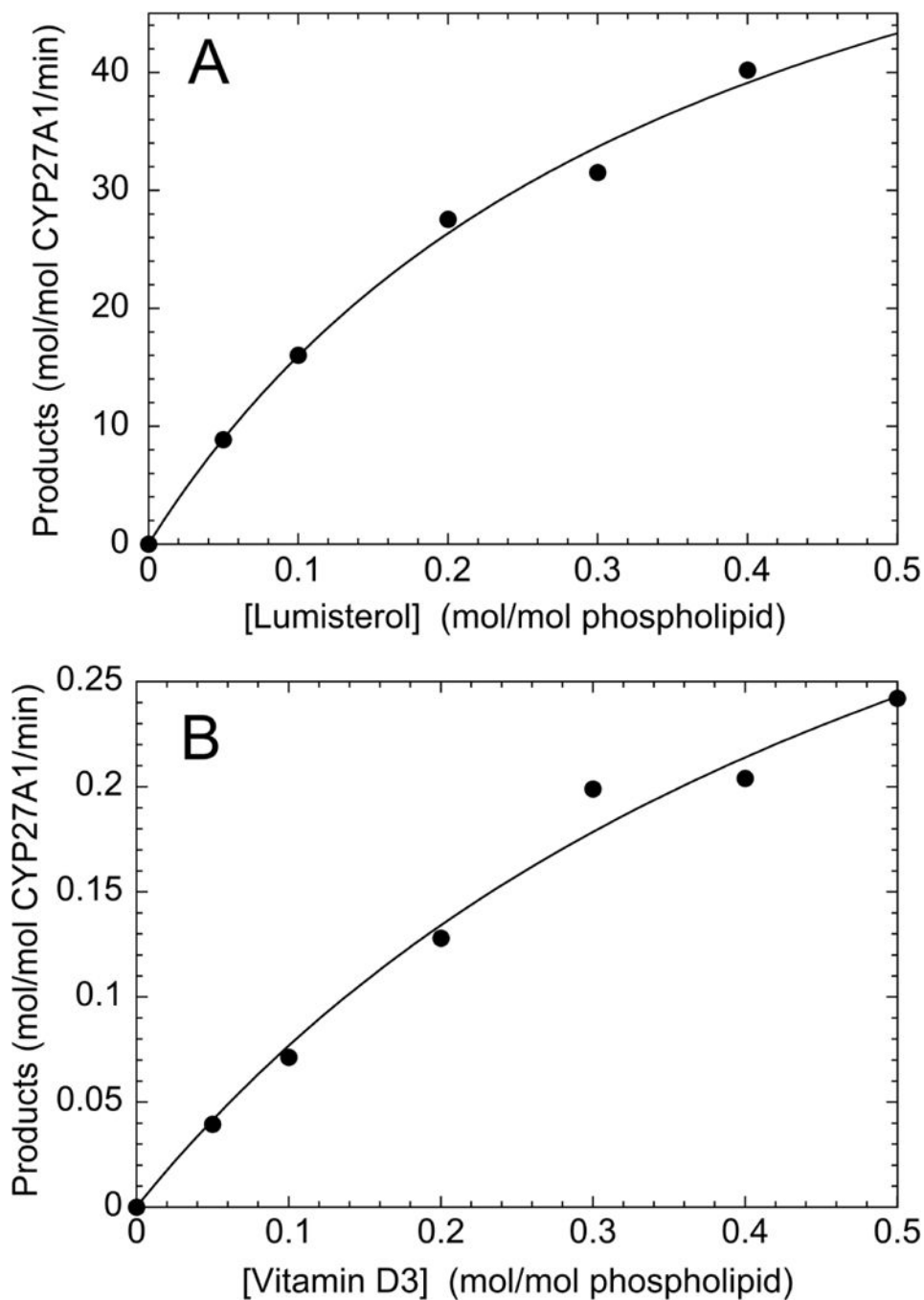


Fig. 5. Comparison of the kinetics of metabolism of L3 and vitamin D3 in phospholipid vesicles. L3 (A) and vitamin D3 (B) were incubated with 0.1 μ M CYP27A1 for 5 min, or 0.2 mM CYP27A1 for 10 min, respectively, as in Fig. 1A. Extracts were analysed by reverse phase HPLC to determine the amounts of products formed. Hyperbolic curves described by the Michaelis-Menten equation were fitted to the data using Kaleidagraph 4.5.2

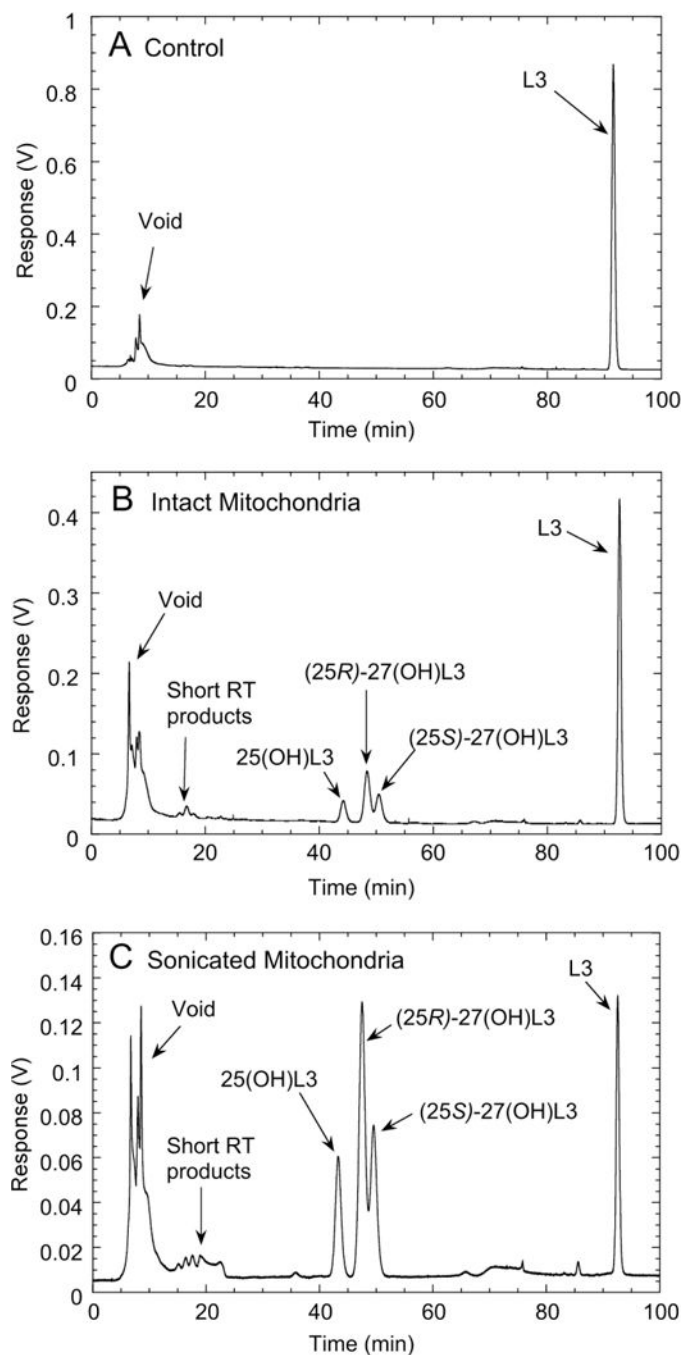
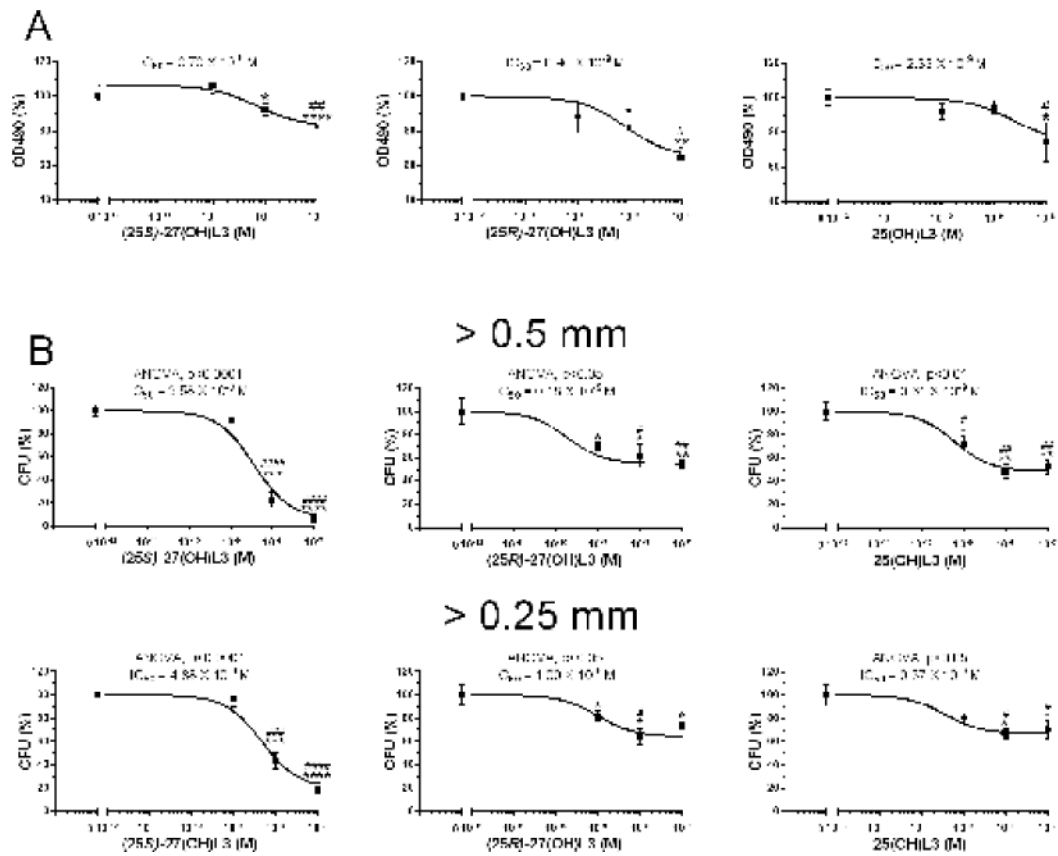


Fig. 6. Metabolism of L3 by mouse liver mitochondria. Liver mitochondria (1.0 mg/ml) were incubated with 28 μ M L3 in 0.45% HP- β -CD (added from a 10 \times stock) in the presence of 5 mM isocitrate and 0.5 mM NADPH, for 1 h at 37 $^{\circ}$ C. Steroids were extracted and analysed by reverse phase HPLC as in Fig. 1. (A), control incubation of intact mitochondria with NADPH and isocitrate omitted. (B), test incubation with intact mitochondria. (C), test incubation with mitochondria disrupted by sonication and supplemented with purified adrenodoxin reductase (0.4 μ M) and adrenodoxin (15 μ M).

**Fig. 7.**

Effect of hydroxylumisterols on SKMEL-188 melanoma proliferation and colony formation.

A, Anti-proliferative activity measured after 72 h of treatment with hydroxylumisterols with

MTS reagent; B, Colony formation. Data represent means \pm SE (n = 3) where *p<0.05,

p<0.01, *p<0.001 and **** p<0.0001 by the student t-test; #p<0.05, ##p<0.01,

###p<0.001 and ####p<0.0001 by one-way ANOVA. General ANOVA tests are shown for

B.

Table 1

Comparison of side-chain chemical shifts of products 2A and 2B with 25(*S/R*)-27-hydroxy cholesterol standard compounds.

Assigned	(25 <i>S</i>)-27-hydroxycholesterol		(25 <i>R</i>)-27-hydroxycholesterol	
	¹³ C (ppm)	¹ H (ppm)	¹³ C (ppm)	¹ H (ppm)
C23	24.4	1.17, 1.43	24.4	1.34
C24	34.7	1.03, 1.43	34.6	1.06, 1.36
Assigned	(25 <i>S</i>)-27-hydroxyL3 (Product 2A)		(25 <i>R</i>)-27-hydroxyL3 (Product 2B)	
	¹³ C (ppm)	¹ H (ppm)	¹³ C (ppm)	¹ H (ppm)
C23	24.6	1.17, 1.46	24.4	1.35
C24	34.7	1.02, 1.45	34.6	1.06, 1.35

Table 2

Metabolism of lumisterol by intact and disrupted mouse liver mitochondria. Incubations of L3 (50 μM) were carried out for 60 min with either intact mitochondria or mitochondria disrupted by sonication. Total products formed were determined from chromatograms as in Fig. 6. Where indicated, adrenodoxin reductase (AR) and adrenodoxin (Adx) were added to final concentrations of 0.4 μM and 15 μM , respectively. Cholestane-triol, 5 β -cholestane-3 α ,7 α ,12 α -triol.

Mitochondria	AR and Adx	Cholestane-triol (μM)	Product (nmol/mg protein)
Intact	-	0	6.0
Intact	-	50	1.1
Intact	-	150	0.63
Sonicated	-	0	0
Sonicated	+	0	16.3
Sonicated	+	50	5.2
Sonicated	+	150	1.7